



# Numerical Simulation of Pullout Behavior of Steel Grid Embedded in Gravels

Siyuan Li<sup>1\*</sup>, Qingyuan Zeng<sup>2</sup>

<sup>1</sup>Department of Geotechnical Engineering, Tongji University, Shanghai 200092, China

<sup>2</sup>China MCC5 Group Shanghai Corp. Ltd., Shanghai 201900, China

\*2132369@tongji.edu.cn

**Abstract.** Steel grid is an effective reinforcement material for improving weak foundations and it is necessary to conduct in-depth research on its mechanism. Finite-discrete coupling method was used for numerical simulation of steel grid pull-out test in gravels. By analyzing the mechanical response of particles and steel grids near the soil reinforcement interface under overburden stress and comparing it with experimental data, it can be seen as an effective method for the simulation of steel grids. During the pulling process, a concentrated displacement zone gradually forms in the vicinity of the steel grid, which drives the soil to move in the pulling direction together. In addition, the contact force chain of the soil is concentrated on the front end, indicating that the friction and bearing resistance of the transverse and longitudinal ribs of the steel grid can significantly improve the interfacial strength.

**Keywords:** steel grid, gravels, DEM-FEM coupling

## 1 Introduction

With the increasing number of large-scale projects constructed on soft soil foundations, it is crucial to improve the bearing capacity of them. Steel grids, as a kind of material with high strength and low elongation rate, can effectively reduce settlement when used as reinforcing material.

Liu<sup>[1]</sup> found through vibration table tests that steel grid reinforcement has a significant effect on the seismic resistance of bridge piers. Lajevardi<sup>[2]</sup> found through pull-out tests that steel grids have higher shear strength compared to ordinary geogrids. Pankaj<sup>[3]</sup> reinforced the embankment with geogrids and steel grids on both sides and found that the lateral displacement and settlement on one side of the steel grid were smaller than those on the other side. Liang<sup>[4]</sup> conducted dynamic tensile tests on steel grids to investigate their tensile behavior. Cwirko<sup>[5]</sup> conducted steel grid pull-out tests in fine sand, demonstrating the effectiveness of low deformation of steel grids in reinforcement. Results from experimental research are intuitive but cannot reveal microscopic features. Ghazavi<sup>[6]</sup> explored the effect of grid reinforcement on soft sand using finite difference software FLAC2D. Pol<sup>[7]</sup> evaluated the reinforcement effect of steel wire mesh in

slopes using discrete element method. However, the finite element method cannot simulate the discrete characteristics of soil well and the discrete element method cannot reflect the continuity of the steel grid as a rigid structure using particles. Besides, most studies mainly focus on sandy soil fillers but not gravels, which have a large number of applications in railway tracks and roadbeds.

Therefore, a discrete-continuous coupling numerical model of steel grid pull-out tests in gravels was established. It was combined with the results of pull-out tests and explored further on its mechanical behavior at the reinforced interface.

## 2 Numerical Model of Steel Grid Pulling Test

Gravels were established with particles in the discrete element software PFC3D based on its discontinuous structural characteristics. Steel grids were made of continuous material and were established with solid elements in the finite difference software FLAC3D. The mutual motion and force between two materials were transmitted through the coupling medium “Wall” and the model through discrete continuous coupling was established to analyze the mechanical behavior during the pull-out test.

### 2.1 Establishment of FEM-DEM coupling model

The model shown in Figure 1 was established based on the actual pull-out test in Figure 2. It was taken as the sample size with length 850 mm, width 400 mm and height 300 mm in the experiment. Based on gravel’s own shape and anti-rolling properties, it was established by using rblocks instead of spherical particles. The grading, parameters of gravels, and parameters of steel grids are shown in Tables 1, 2, and 3, respectively. An overburden stress of 30 kPa was applied through the upper wall after sample formation, and a certain speed was set at the front end of the steel grid to pull it out, with a total pulling displacement of 20 mm.

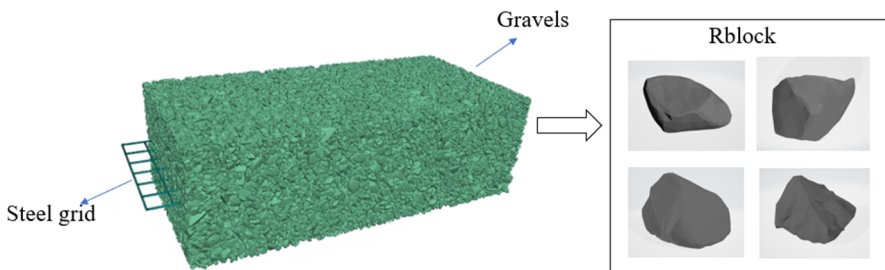


Fig. 1. Numerical model



**Fig. 2.** Steel grid pull-out test

**Table 1.** Gradation of gravels.

Type of packings	Particle diameter (mm)	Percentage (%)
Gravels	0—9.5	52
	9.5—19	23
	19—31.5	25

**Table 2.** Microscopic parameters of gravels

Type of packings	Density (kg/m <sup>3</sup> )	friction coefficient	Effective modulus(MPa)	Stiffness ratio	Number of particles
Gravels	2650	0.35	100	1.5	46192

**Table 3.** Microscopic parameters of steel grids

Type of material	Cross-sectional area(mm <sup>2</sup> )	Effective modulus (GPa)	friction coefficient	Poisson's ratio
Steel grid	7	50	0.35	0.3

## 2.2 Verification of Numerical Model

The results calculated using the above microscopic parameters were compared with the monitoring data of the actual pull-out test, as shown in Figure 3. By comparing the pull-out force-displacement curve, the numerical simulation results are well consonant with the experimental results and are basically consistent.

At the beginning of the experiment, when the pull-out displacement was small, the pull-out force increased rapidly with the increase of displacement, approaching linear growth. However, in the later stage of the experiment, the corresponding curves gradually slowed down as the pull-out displacement increases, until the end of the experiment, when the pull-out force reached its peak. Under an overburden stress of 30 kPa, the ultimate pull-out force of steel grid in gravels reached 20 kN, which is much greater than that of conventional geogrids.

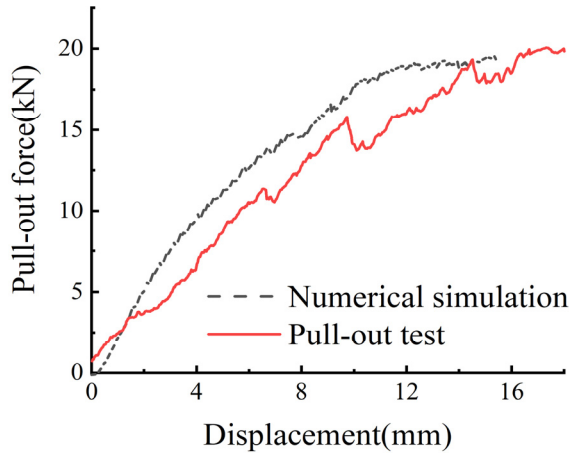


Fig. 3. Results from numerical simulation and pull-out test

### 3 Analysis of Numerical Result

#### 3.1 Displacement Field

Figure 4 shows the displacement field cloud map of the middle section of the sample under different pulling displacements. It can be seen that a concentrated displacement zone gradually formed in the vicinity of the steel grid. The displacement at both ends of the sample was relatively small, while the displacement of the gravels near the steel grid was relatively large. As the pull-out displacement increases, this phenomenon became more pronounced. It can be explained that the frictional force between the ribs of the steel grid and the soil, as well as the passive resistance on the transverse ribs, will drive the soil to move together in the direction of pulling.

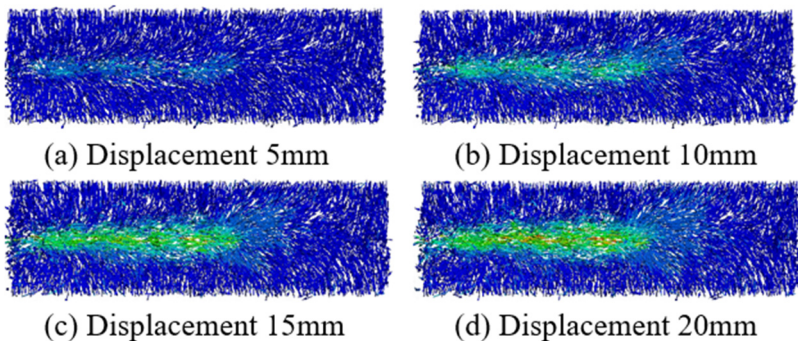


Fig. 4. Displacement field of gravels in each stage of pulling

As the pulling process progressed, the soil at the front end was compressed but could not be squeezed out from the narrow gap, resulting in some vertical movement along

the left wall. At the end of the steel grating, the steel grid moved to the left and a cavity was generated at the end, and the nearby soil moved towards the cavity under the action of compression. Due to the influence of gravity, the displacement of the upper and lower parts of the gravel was not uniform, and the movement of the upper soil was greater than that of the lower soil. Under the above effect, it can be observed that the displacement field of the upper soil of the sample generally has a clockwise rotation trend, while the displacement field of the lower soil has a counterclockwise rotation trend.

### 3.2 Contact Force Chain

The thickness and density of the force chain in Figure 5 can determine the distribution of contact force. In the initial stage of pulling, the distribution of contact force chains was relatively uniform. As the pulling progresses, the steel grid moved to the left, and the contact force chain gradually concentrated at the front end of the grids. This indicates that there was more interaction between the steel grid and gravel particles, and the embedding effect between them made the interlocking effect of the gravels stronger. At the same time, it also increased the frictional force and passive resistance between gravels and ribs of the steel grid.

If only the contact force between the gravels and the steel grids, the contact numbers between them are 1192, 1357, 1363, and 1456, respectively, when the pull-out displacement reaches 5 mm, 10 mm, 15 mm, and 20 mm. Similar to the overall force chain law, as the pulling displacement increases, the strong chain concentrated at the front end, indicating that there was more interaction between the steel grid and the gravel particles.

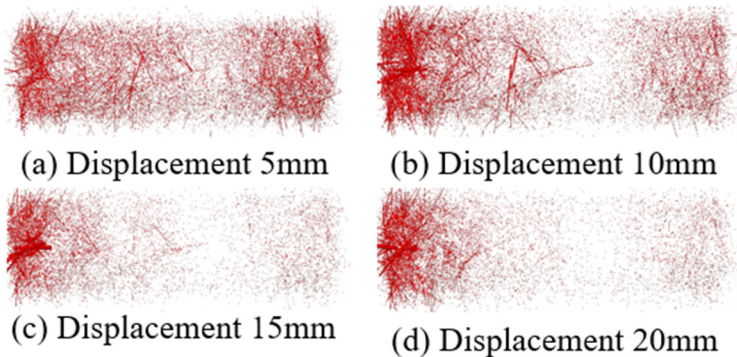


Fig. 5. Contact force chain of gravels in each stage of pulling

## 4 Conclusion

A FEM-DEM coupling model for steel grid pull-out test in gravels is established, which takes into account both the continuous characteristics of steel grids and the discrete

characteristics of gravels. By comparing and verifying with experimental data, the corresponding relationship between macro and micro parameters of the steel grid pull-out test is obtained, providing an effective and reliable model reference for subsequent numerical analysis and research. During the steel grid pulling process, there was a significant displacement field generated by gravel particles near the steel grid, which moved in the pulling direction with the grids. The stress in the soil gradually concentrated towards the tensile end, forming a strong chain at the front end.

The model demonstrates the strengthening effect of steel grid transverse and longitudinal ribs in reinforced soil and can be applied in engineering design to select the optimal steel grid reinforcement system through numerical calculations during foundation reinforcement. The separate roles of longitudinal and transverse ribs were not discussed here, and further research can be conducted in this area.

## References

1. Liu, Z., Chen, X., Zhang, X., Ding, M., Lu, J., Tang, J, (2023) Effect of steel grid on enhancing seismic performance of bridge pier with low reinforcement ratio: Shaking table test and numerical simulation. *J. Structures*,57: 105211. 10.1016/j.istruc.2023.105211
2. Mirzaalimohammadi, A., Ghazavi, M., Lajevardi, S.H., Roustaei, M. (2019) Laboratory studies of interaction properties between fine sand and various grid reinforcements *J. Innovative Infrastructure Solutions*,4(1):48. 10.1007/s41062-019-0235-y
3. Pankaj, B., Dennes, T.B., Sowarapan, D. (2016) The use of polymeric and metallic geogrid on a full-scale MSE wall/embankment on hard foundation: a comparison of field data with simulation. *J. International Journal of Geo-Engineering*, 7(1): 29. 10.1186/s40703-016-0035-6
4. Liang, L., Wenli, L., Jun, W., Wenjie, W., Meng, W. (2021) Experimental Investigation on Dynamic Tensile Behaviors of Engineered Cementitious Composites Reinforced with Steel Grid and Fibers *J. Materials* ,14(22): 10.3390/ma14227042
5. Ówirko, M., Jastrzębska, M. (2021) Behaviour of the steel welded grid during a simplified pullout test in fine sand. *J. Applied Sciences (Switzerland)*, 11(19): 10.3390/app11199147
6. Ghazavi, M., Foghani, P., Moghaddam, P. T. (2024) Stochastic analysis for bearing capacity computation of twin strip footings on geogrid-reinforced sands. *J. Georisk: Assessment and Management of Risk for Engineered Systems and Geohazards*: 10.1080/17499518.2024.2316263
7. Pol, A., Gabrieli, F. (2021) Discrete element simulation of wire-mesh retaining systems: An insight into the mechanical behaviour. *J. Computers & Geotechnics*, 134: 104076. 10.1016/j.compgeo.2021.104076

**Open Access** This chapter is licensed under the terms of the Creative Commons Attribution-NonCommercial 4.0 International License (<http://creativecommons.org/licenses/by-nc/4.0/>), which permits any noncommercial use, sharing, adaptation, distribution and reproduction in any medium or format, as long as you give appropriate credit to the original author(s) and the source, provide a link to the Creative Commons license and indicate if changes were made.

The images or other third party material in this chapter are included in the chapter's Creative Commons license, unless indicated otherwise in a credit line to the material. If material is not included in the chapter's Creative Commons license and your intended use is not permitted by statutory regulation or exceeds the permitted use, you will need to obtain permission directly from the copyright holder.

